

# EFFECT OF FINES CONTENT ON LIQUEFACTION RESISTANCE DURING STEADY-STATE CONDITIONS

\*Hanindya Artati<sup>1</sup>, Widodo Pawirodikromo<sup>1</sup>, Paulus Rahardjo<sup>2</sup>, and Lalu Makrup<sup>1</sup>

<sup>1</sup>Faculty of Civil Engineering and Planning, Universitas Islam Indonesia, Indonesia; <sup>2</sup>Faculty of Engineering, Universitas Katholik Parahyangan, Bandung.

\*Corresponding Author, Received: 8 June 2022, Revised: 1 May 2023, Accepted: 29 May 2023

**ABSTRACT:** Liquefaction takes place in a large strain with constant stress and at a constant volume, known as steady-state conditions. Liquefaction also occurs in sandy soils with fine grain content, which affects the relative density and uniformity coefficient. Palu City is an area severely affected by the liquefaction phenomenon after the 2018 Central Sulawesi earthquake. Thus, a series of studies are needed to determine liquefaction susceptibility at steady-state conditions with the influence of variations of fine-grained content. This research was conducted by analyzing the grain size distribution and the influence of fine grain content that affected the relative density and uniformity coefficient at steady-state conditions to obtain the value of cyclic liquefaction resistance. The tests were carried out in a laboratory in the form of grain size distribution analysis, proctor standard, and triaxial consolidated undrained using sand with a fines content of 2%, 5%, 9%, 13%, and 17%. The study revealed that the sand of Palu City, based on grain gradation, is in the most liquefiable soil range. Moreover, with the addition of the fines content, the higher the  $C_u$  value, the larger the range and the more diverse the grains. These results strengthen the undrained strength of the sand under axial load at steady-state conditions. In conclusion, the gradation will affect the void ratio and the critical-state line.

*Keywords: Fines content, Uniformity Coefficient, Silty sand, Steady-states, Cyclic liquefaction resistance, Critical state line.*

## 1. INTRODUCTION

Earthquakes generate vibrations that occur in the soil layers caused by the movement of tectonic plates. Earthquakes release energy propagated by the hypocenter in the form of primary waves (P waves) and secondary waves (S waves). The propagation of S waves will generate an alternating shear force, which propagates from the bedrock to the surface in the form of peak ground acceleration, which with a relative density of more than 75%, will increase the vertical stresses. In some studies, the method of determining the maximum likelihood was used in determining the a-b value of the Gutenberg-Richter relation [2], [3], in which the results obtained are based on the fault distance and maximum magnitude of several return periods.

The value of  $a_{max}$  on the surface was determined based on earthquake data in 1923-2021 with a radius of 500km, as presented in Figure 1, using Probabilistic Seismic Hazard Analysis (PSHA). In this case, the peak acceleration value of the time history of acceleration in bedrock was 0.44g for earthquakes with a probability of exceeding 2% in 50 years [4], [5], while the peak acceleration in the time history of acceleration at the surface increased to 0.807 g with an earthquake probability of exceeding 2% in 50 years [6]. This surface acceleration is one of the factors that affect the

vulnerability of the soil to liquefaction [7]. If the cyclic resistance ratio of the dynamic force exceeds the shear resistance of the soil, it will trigger the collapse of the soil and result in liquefaction.

Liquefaction is known to cause a very broad impact, making it important to carry out an assessment of the risk of post-earthquake damage as a mitigating factor for a certain return period [8]. In this study, an effective stress analysis was carried out to examine the relationship between soil particle interactions and pore water pressure, especially at steady-state conditions. The phenomenon of liquefaction occurs in many types of sandy soil because it is cohesionless. Based on the Palu Earthquake, the Center of Sulawesi [9] showed an increase in weatherable minerals in the sand fraction, thus identifying an increased vulnerability to liquefaction hazards in the next return period.

Soil resistance to liquefaction is inseparable from the distribution of particles in pure sand to silty sand [10], which is caused by the percentage of fine fraction content. Soil density which is interpreted as relative density ( $D_r$ ) indicates the different distribution of sand grains based on the percentage of sand grain content and fines content. This affects the value of the Uniformity Coefficient ( $C_u$ ) and curvature coefficient ( $C_c$ ), [11].

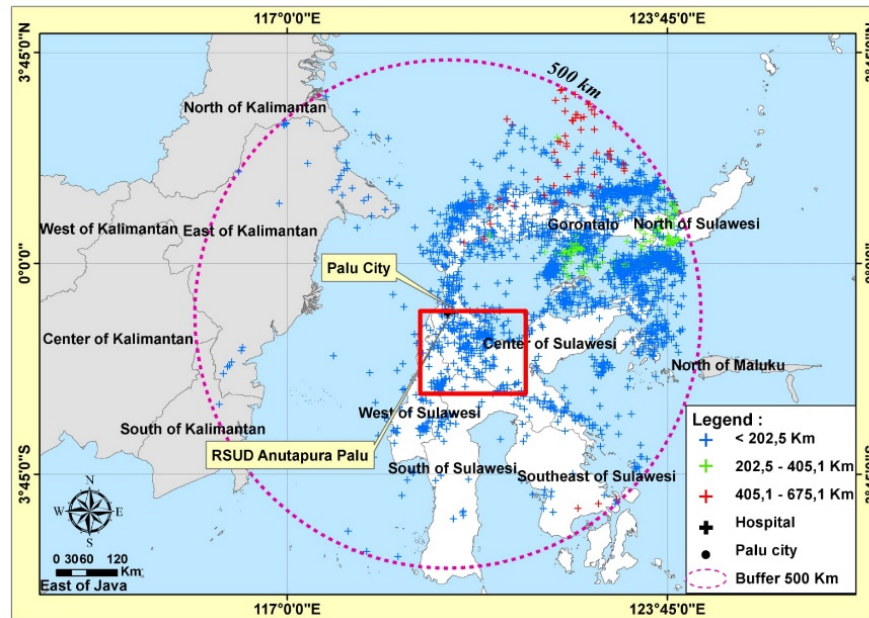


Fig. 1. Distribution of earthquake epicenters for palu city and surrounding areas from 1923-2021 (modified from the zmap program)

The extent to which the effect of fines content [12] affects soil density ( $D_r$ ) [13], [14], in loose to dense conditions, will cause changes in the value of cyclic liquefaction resistance and form a critical state trendline. Soil density with grain distribution in sandy soil will bring the soil to a critical state line [15] when it is stressed by a sufficiently large strain at a constant volume [16]. The critical state line for granular soils can be obtained from a series of triaxial consolidated undrained (C.U.) tests. [17]. The triaxial C.U. test with different relative densities and certain fines content reveals the behavior of silty sandy soils on a critical state line, which can be used as a future reference in determining soil vulnerability due to liquefaction phenomena. Steady-state conditions are indicated when the soil obtains constant stress and a constant volume at a sufficiently large strain [18].

Previous research demonstrated the need to conduct more specific research to enrich and complement the previous literature, as well as new breakthrough research on the effect of the combination of fines content (F.C.), in determining the critical state line on the value of cyclic liquefaction resistance on native soils in Palu City with a value of surface peak acceleration ( $a_{max}$ ) obtained from Probabilistic Seismic Hazard Analysis (PSHA).

## 2. RESEARCH SIGNIFICANCE

The results of this study are expected to contribute to the mitigation of the liquefaction phenomenon due to the earthquake. In addition, by obtaining the critical state line, it will be easy to

determine whether a condition has the potential for liquefaction. The determination of the maximum acceleration on the surface was carried out based on the determination of the value of  $a-b$  in the Gutenberg-Richter relation as the determination of the value of cyclic liquefaction resistance. A series of laboratory experiments such as sieve distribution analysis, proctor standard and triaxial tests will show the extent to which soil behavior is affected by relative density and grain distribution on fine content variation so that it can describe the change in the critical state line on the fine grain variation. These results would disclose the actual behavior of the soil at steady-state conditions and the effect on soil susceptibility due to the liquefaction phenomenon.

## 3. EXPERIMENTS OVERVIEW

This research began with the analysis of the distribution of soil grains and their relative density on the fines content and its effect on cyclic liquefaction resistance. Thus, an experiment was carried out in the laboratory using consolidated undrained triaxial test to determine the behavior of the soil under steady-state conditions until a critical state line was obtained as a reference. The research implementation is described as follows.

### 3.1 Specimen Preparation

The specimen had a height of 70 mm and a diameter of 35 mm. Prior to shearing, the specimen went through the stages of saturation and consolidation. In this study, the specimens were

prepared in different densities and were placed between the pore stones, then coated with a membrane and locked using an o-ring.

The saturation process is an important process in which the specimen of the test approaches the condition of the perfect saturation degree before shearing. To achieve a perfect degree of saturation which is elastic and isotropic, the result is calculated using the Skempton's coefficient (coefficient of pore water stress), assuming the specimen consists of solid and liquid. Saturation is the ratio between the volume of water and the volume of voids, Referring to Eq. (1).

$$S_r = \frac{v_w}{v_v} \quad (1)$$

While Skempton's Value (B), Refer to Eq. (2), (3) and (4).

$$\Delta u = B(\Delta\sigma_3 + A(\Delta\sigma_1 - \Delta\sigma_3)) \quad (2)$$

$$\Delta u = B\Delta\sigma_3 + AB(\Delta\sigma_1 - \Delta\sigma_3) \quad (3)$$

$$\Delta u = B\Delta\sigma_3 + \bar{A}(\Delta\sigma_1 - \Delta\sigma_3) \quad (4)$$

The compression phase is performed; refer to Eq. (5),

$$\Delta u = B \cdot \Delta\sigma_3 \quad (5)$$

The soil sample had reached perfect saturation if the B value was 1.0 or close to 98% saturation level.

Loose specimens, upon the completion of the saturation stage, were then proceeded to the following consolidation stage [26], where the specimens were subjected to circumferential stress and axial stress at a constant rate of 0.5%/min in axial strain ( $\epsilon_a$ ), with the drain valve closed. This was due to the fact that the test was planned to stretch 20% at  $t_f$  time, so the speed of motion was calculated with Eq.6.

$$v = \frac{(\epsilon \times H)}{(100 \times t_f)} \quad (6)$$

Vertical motion velocity was ( $v$ ) (mm/min),  $\epsilon$  was the strain (%),  $t_f$  was the failure time which - depended on  $t_{100}$ , and it was the time required to reach 100% consolidation (minutes). It used a minimum failure time  $t_f$  of 120 minutes to C.U. triaxial test, while  $H$  was the height of the object of soil test (mm).

The pore water pressure balance during shear was verified at the top and bottom of the specimen. The shear test would be stopped after the axial strain reached about 20% and a value of  $q_{max}$  is obtained, which was defined as the maximum shear strength over the axial strain range. Based on [22], failure due to shear would occur in one of the failure models in Figure 2, namely 2(a) barreling, 2(b) slipping and barreling and 2(c) slipping.

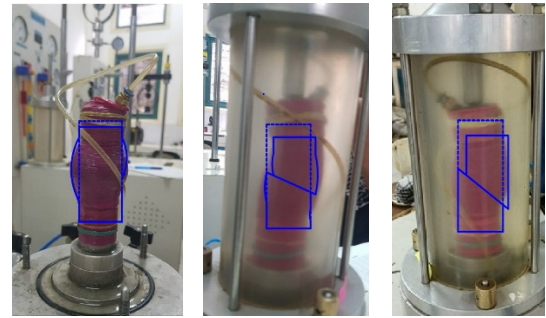


Fig. 2 (a) Barreling (b) Barreling Slipping (c) Slipping.

The correction area can also be determined based on the graph in Figure 3 on the amount of strain experienced by the sample. Based on [27], it was obvious that in the undrained triaxial test, the shear strength ( $S_u$ ) would increase in line with the increase in fine contents, which was related to the friction that occurred in the sand soil content.

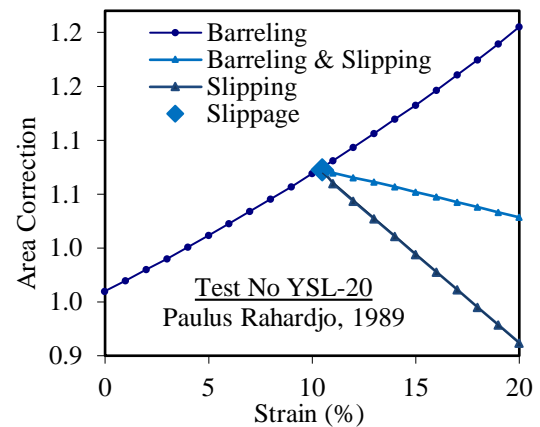


Fig. 3 Area correction (Rahardjo, 1989).

### 3.2 Standard Proctor Compaction Test Program

The research was conducted on the native soil samples from Palu City, Central Sulawesi, with fines content of 0% to 20%. In observing the relationship between relative density and grain distribution, soil samples were grouped into soil samples with a fines content of 2%, 5%, 9%, 13% and 17%.

The experiment was carried out at the Soil Mechanics Laboratory, Universitas Islam Indonesia and Catholic Parahyangan of University, Bandung. It was commenced by testing the Standard Proctor in order to obtain the Optimum Moisture Content value for each soil content and continued with a sieve and triaxial distribution analysis in unconsolidated undrained conditions.

The standard proctor test refers to [19], and was carried out on five samples, with different fine grain

contents of 2%, 5%, 9%, 13% and 17%. The varying fines content of 2%, 5%, 9%, 13% and 17%, generated the optimum moisture content as presented in Figure 4. The test results show the greater the fines content, the greater the OMC value to achieve Maximum Dry Density (MDD).

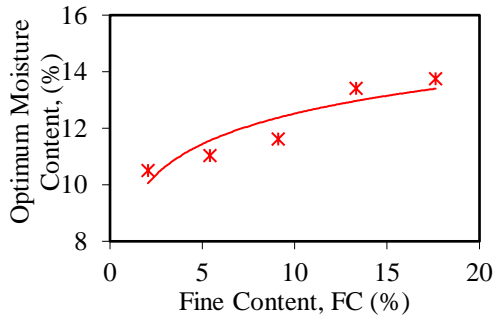


Fig. 4 Optimum moisture content of silty sand with variations in fines content

### 3.3 Grain Size Distribution

Assessment of liquefaction potential can be

done based on the analysis of the sieve distribution, plotted into the Tsuchida range [20]. These results obtained a soil grain distribution curve that can estimate the vulnerability of the soil to potential liquefaction.

The distribution of soil grains indicated that the boundaries of the soil grain distribution in the boundary conditions for most liquefiable soil were the boundaries for the most potentially liquefiable soil and the boundaries for potentially liquefiable soil was the boundaries for potentially liquefiable soil boundaries for potentially liquefaction soils.

The sieve analysis and hydrometer analysis were conducted to obtain grain size distribution [21]. The analysis was carried out from the results of the grain size distribution test to determine the silt content in the sandy soil, as well as the distribution of the particles consisting of a combination of sand and silt. The grain size analysis shows the combination of soil-dominated and fine sandy soil. It shows in Figure 5.

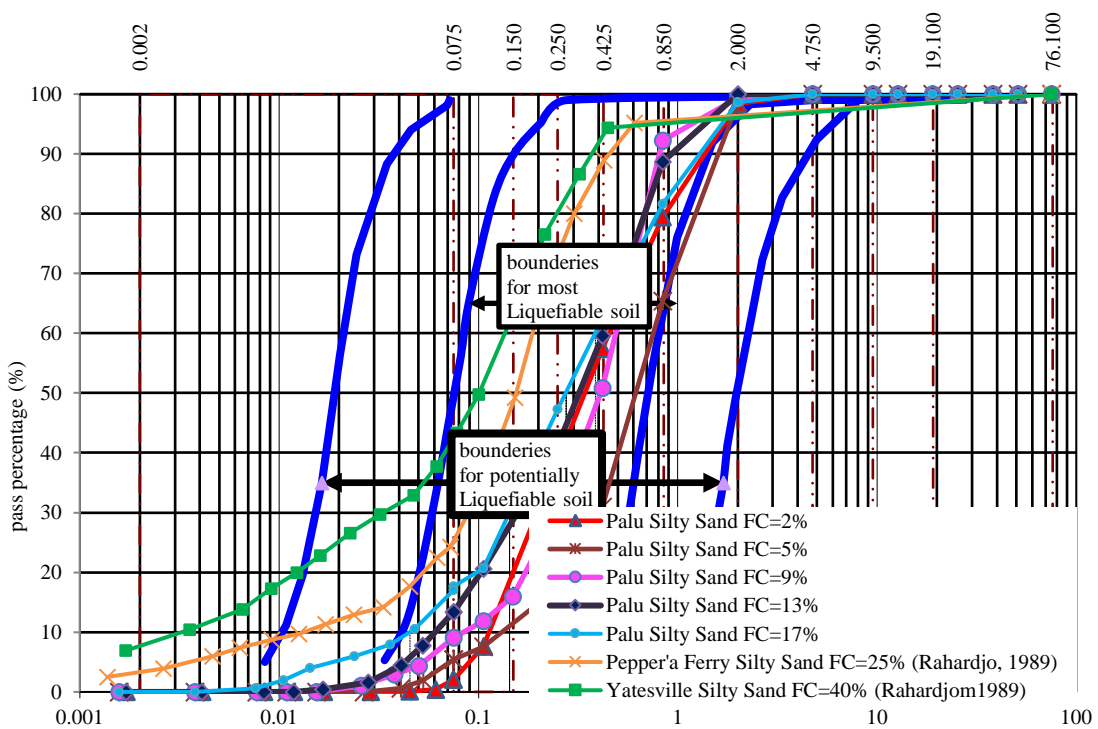
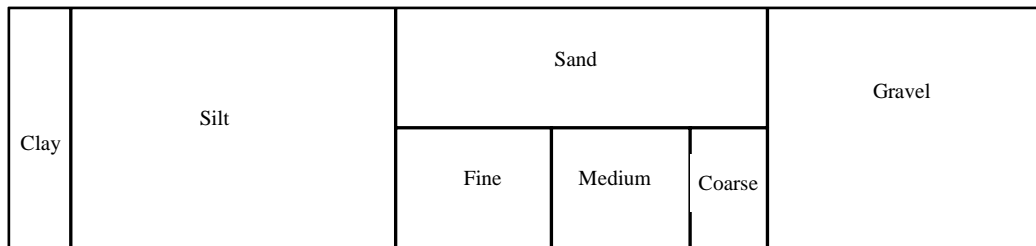


Fig. 5 Gradation of silty sand grains against the Tsuchida curves, 1970

The results of the grain size graph determine the uniformity coefficient (Cu) shows the size range of soil grains in Figure 6.

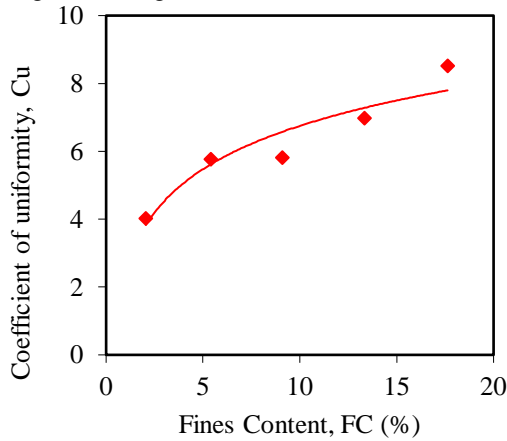


Fig. 6 Relationship between fines content and uniformity coefficient in potential liquefaction soil

The larger Cu value indicates that the soil grain size varies or the soil is well-graded. Meanwhile, the Cu value of < 4, or the smaller the Cu value, the more the same grain size (poorly graded). This can be approximated by the fine soil content contained in the sand, where the greater the value of the fines content, the higher the Cu value, Figure 7.

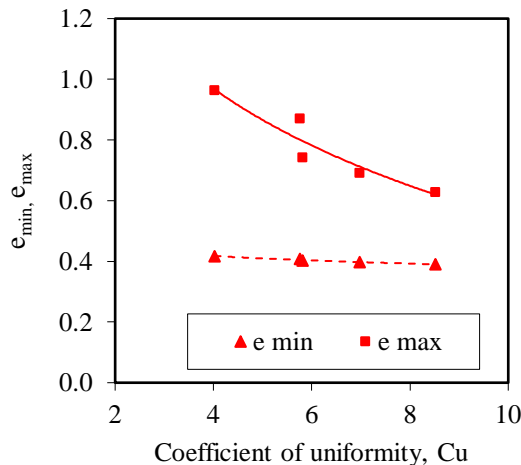


Fig. 7 Variation in the maximum (e<sub>max</sub>) and minimum (e<sub>min</sub>) void ratios of coefficient uniformity and coefficient curvature

Meanwhile, the curvature coefficient (Cc=1) had a well-graded grain size distribution. As for the value of the curvature coefficient (Cc < 1 or Cc > 1), the grain size of the soil was only limited to large or small sizes, and thus it was called a soil void of a complete grain size variation (gap graded). The graph shows a fines content of 2% Cc=0.75 and for fines content > 2% have Cc>1 (Table 1).

Table 1 Value of Uniformity Coefficient (Cu) and Coefficient of Curvature (Cc)

FC(%)	2%	5%	9%	13%	17%
e <sub>min</sub>	0.44	0.40	0.35	0.31	0.27
e <sub>max</sub>	0.96	0.87	0.74	0.69	0.63
Cu	4.02	5.76	5.82	6.97	8.52
Cc	0.75	1.66	1.48	0.96	1.17
Cc/Cu	0.19	0.29	0.25	0.14	0.14

The variation of the Silty Sand soil sample with silt content of 2%, 5%, 9%, 13% and 17%, in Figure 6, depicts that the soil grain distribution curve is at the limit of very potential for liquefaction, where the sand soil consists of silt particles and finer particles smaller than 0.074 millimeters, which pass through the openings in the US Standard sieve No. 200 and layered with the gradation curve of Rahardjo's research [22] from Yatteville Silty Sand and Pepper's Silty Sand, with fines content of FC=25% and FC=40%.

It is clear that the fines content will affect the relative density of the soil, which is indicated by the value of the void ratio (e), Figure 8.

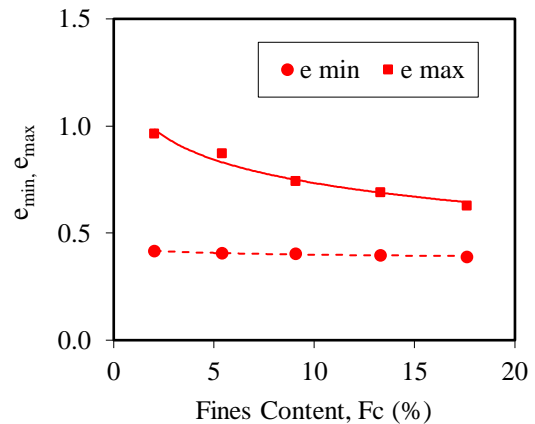


Fig. 8 The variation of fines content (F.C.) to maximum void ratio (e<sub>max</sub>) and minimum void ratio (e<sub>min</sub>),

Cubrinovsk M., and Ishihara K (2002) [23] in his research explain if pure sand and sand with fine soil also affect the value of the unit weight of the soil in dry conditions. The addition of nonplastic fine soil content in the poorly graded sand grains will decrease the value of the void ratio so that the dry density will increase.

The results show the relationship between the void ratio and the material properties of the sand. Hence, the grain size distribution can represent gaps in soil gradation to obtain e<sub>max</sub> and e<sub>min</sub> values in the laboratory. The fines content versus dry density (γ<sub>d</sub>) can see in Figure 9.

To examine the liquefaction behavior of sandy or silty sand, several parameters such as void ratio, uniformity coefficient, and relative density can be used. This study tried to display the different relative densities of each specimen for different fine contents, as depicted in Figure 10.

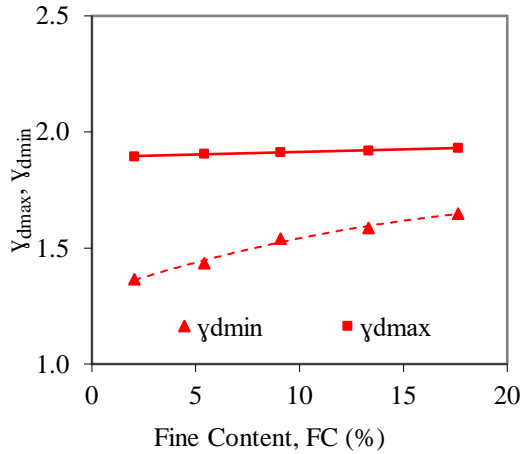


Fig. 9 The variation of fines content (F.C.) to maximum dry density ( $\gamma_{dmax}$ ) and minimum dry density ( $\gamma_{dmin}$ )

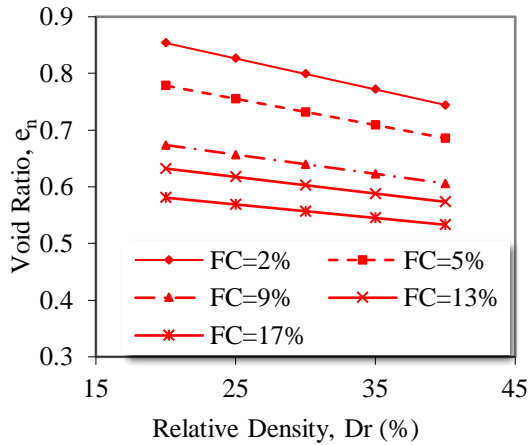


Fig. 10 Relationship between void ratios and relative density in silty sands with variations of fines content

In the case of liquefaction hazard, the soil containing fine grains with low plasticity tends to have greater resistance than the sand content of more than 10% as that of pure sand at the same N-SPT value [24].

### 3.4 Triaxial Test Program

The shear test was carried out using Consolidated Undrained Static Triaxial Test, referring to the test [25]. The sample was the native soil from Palu City with various variations of fine soil content.

The stress-strain correlation in specimens 1 to 5 was labeled as Sample-1(SS-1) to Sample-5(SS-5). The specimens SS-1 to SS-5 had silt content of 2%, 5%, 9%, 13% and 17%, respectively, and thus the test objects were made with different density levels in order to observe the potential behavior of the soil while being shifted.

The relationship between stresses and strain in each sample is presented in Figure 11.

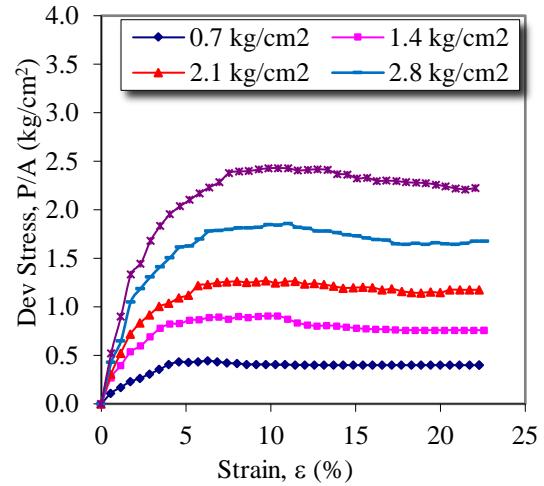


Fig. 11 The stress-strain for consolidated undrained tests on silty sand

The pore water pressure will be constant when the strain is large enough and the soil is in a steady state condition. The relationship between pore water pressure and strain in each sample is presented in Figure 12

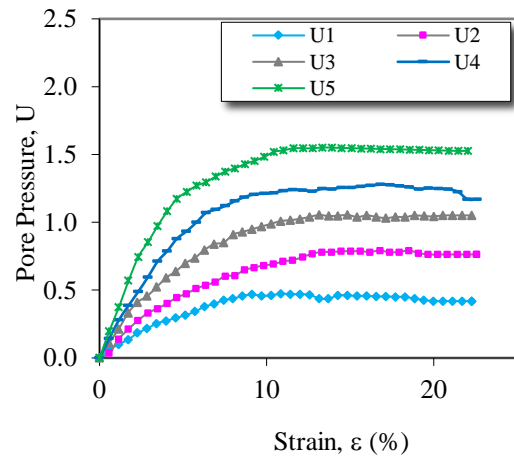


Fig. 12 The pore pressure for consolidated undrained tests on silty sand.

## 4. RESULT AND DISCUSSION

The laboratory testing will be known that soil behavior due to the addition of fines content is affected by the level of density in steady-state conditions. This behavior reveals the shape of the relationship between the uniformity coefficient, fines content, and the level of soil sand resistance to liquefaction. In addition, it will be revealed the behavior of the sample in the steady state condition when the strain is large enough, up to 20%, together with the pore water pressure that influences it during the undrained condition. This study has never been conducted for soil conditions with <20% fines content, especially in the Palu region. By

obtaining the critical steady-state trendline for the soil characteristics of Palu City, Central Sulawesi, Indonesia, the liquefaction resistance value can be determined.

**4.1 Result of Influence of uniformity coefficient on cyclic liquefaction Resistance.**

The original soil sample of Palu City, Central Sulawesi, contained fines content ranging from 0% to 20%, and not more than 20%. The uniformity coefficient (Cu) depends on grain size diameter at sixty percent divided when ten percent, which is not less than 10. The relative density (Dr) was less than 75 %.

Therefore, it was classified as soil with a tendency to have the potential for the occurrence of liquefaction. The larger the percentage of fine sand, the less the resistance to liquefaction. However, the higher the silty percentage of the fine sand, the higher the level of resistance. That behavior is similar when at void ratio conditions and (N1)60, [28]. This can be seen from the value of the uniformity coefficient on cyclic liquefaction resistance, see Figure.13.

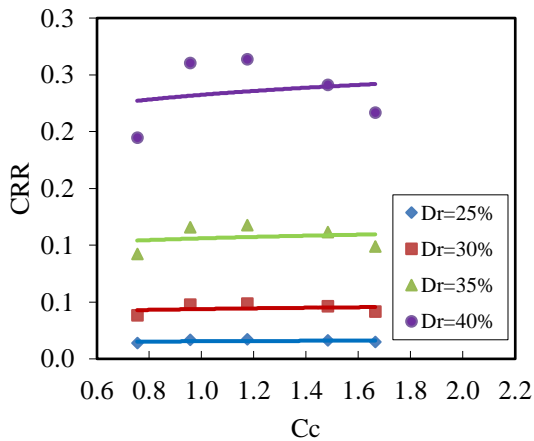


Fig. 13 Relationship between cyclic resistance ratio to uniformity coefficient

Sandy soil mixed with fine soil content at the same Cu value provided higher liquefaction resistance at a greater relative density, and thus it resulted in a different soil behavior. Even though it was only in a narrow range, the increase in resistance to liquefaction was between 0.014 – 0.263.

**4.2 Influence of fines content on cyclic liquefaction Resistance.**

This study investigated the effect of different nonplastic fine-grained soils on cyclic liquefaction resistance. Base sand was obtained from Palu City with silt content of 2%, 5%, 9%, 13% and 17%. It was a particle passing sieve No. 200 (0.074 mm) of

the specified relative density and would obtain a cyclic relationship of resistance to liquefaction, which increased with the fine soil content up to < 20%, [29].

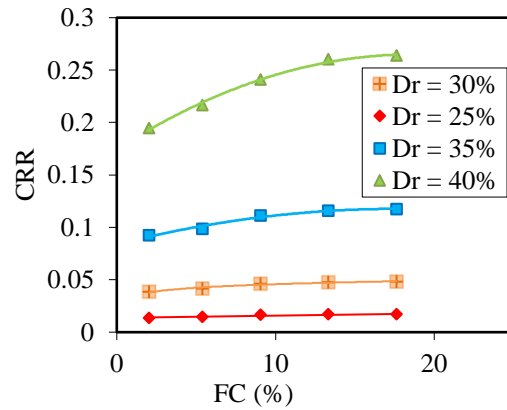


Fig. 14 Cyclic Resistance Ratio (CRR) to sandy soil with varying fines content, at Dr=25%, Dr =30%, Dr=35% and Dr=40%.

Increasing Cyclic Resistance Ratio (CRR) to increasing fine sand content, as shown in Figure 14, it can be observed that clean sand content or sand with 2% F.C. content has a low resistance to liquefaction.

This is attributed to the fact that the fine sand grains have a smaller and/or more uniform average grain size. Meanwhile, the distribution of grains with a larger range (Cu=8,520) in the sand with a fine soil content of 17% will have a high resistance to liquefaction at different or greater relative densities.

Such a condition results from the fact that the average grain size of the sand is getting bigger and/or the sand has a relatively good gradation. Thus, the higher the value of resistance to liquefaction, the higher the increase in the content of fine sand and the increase in the relative density of sand. In monotonic or cyclic loading, the stress-strain in saturated sand is very dependent on the relative density of the sand [30].

**4.3 Results of Triaxial Consolidated Undrained Monotonic Response of Silty Sand**

On the other hand, the behavior of silty sand during the Triaxial test indicated that the strain softening behavior was between contractive/dilative, with the maximum shear stress being reached before deformation occurred at steady state conditions. The results of the triaxial consolidated undrained test showed that the shear stress and excess pore water pressure would be constant when the strain was large or at steady state conditions. The soil behavior of maximum shear stress and steady-state shear stress is depicted in Table 1.

No	Code	Modelling	Soil Behaviour	Peak Condition		Steady State Condition	
				$\tau_{max}$ (kg/cm <sup>2</sup> )	$\epsilon_{max}$ (%)	$\tau_{ss}$ (kg/cm <sup>2</sup> )	$\epsilon_{ss}$ (%)
1	SS-1	strain-softening	contractive	0.442	6.29	0.399	19.43
2	SS-2	strain-softening	contractive	0.907	10.42	0.760	19.68
3	SS-3	strain-softening	contractive	1.269	9.72	1.175	20.58
4	SS-4	strain-softening	contractive	1.858	11.02	1.675	22.04
5	SS-5	strain-softening	contractive	2.429	10.45	2.225	22.06

Table 1: Soil Behavior in Palu City, Anutapura Hospital, Central Sulawesi, Indonesia

During the shearing process, the test object indicated an increase in pore water pressure with positive  $u$ , and a stable response of the deviatoric stress was seen. The relationship of the occurring liquefaction resistance was observable when interpreted at positive excess pore water pressures. When a positive excess pore pressure result ( $\Delta u = +$ ) was obtained, there was a low level of soil resistance to liquefaction, as delineated in Figure 15

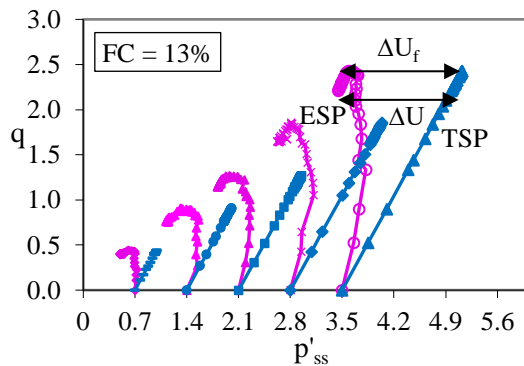


Fig. 15 Pore water pressure from graph of total stress path (TSP) and effective stress path (ESP) at fines content of 13% SS-1

The pore water pressure,  $\Delta u$ , is the difference between the total stress path (TSP) and its effective stress (ESP), [32]. The pore water pressure is formed from changes in the total stress ratio [33], such as an increase in pore water pressure to an increase in total stress, called the pore pressure

parameter, in an oedometer test on saturated soils.

Figure 16 shows soil behavior at effective peak conditions will direct the stress path to a line with a yield internal friction angle of  $\phi'_{peak} = 33.78^\circ$ , and soil behavior in steady state conditions will direct the stress path to one line, with a steady state internal friction angle of  $\phi'_{cv} = 32.75^\circ$ .

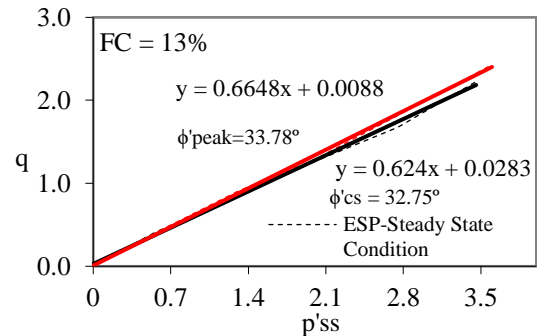


Fig. 16 The effective internal friction angle and the steady-state internal friction angle on the stress path diagram at steady state

During the shearing process on the sample soil to steady-state conditions, the void ratio and mean effective stress will direct the soil sample to a constant volume condition and at constant stress, which forms a straight line called the steady-state line. The line will form a slope angle ( $\lambda_{ss}$ ), which obtains the state parameter value ( $\psi$ ), Figure 17.

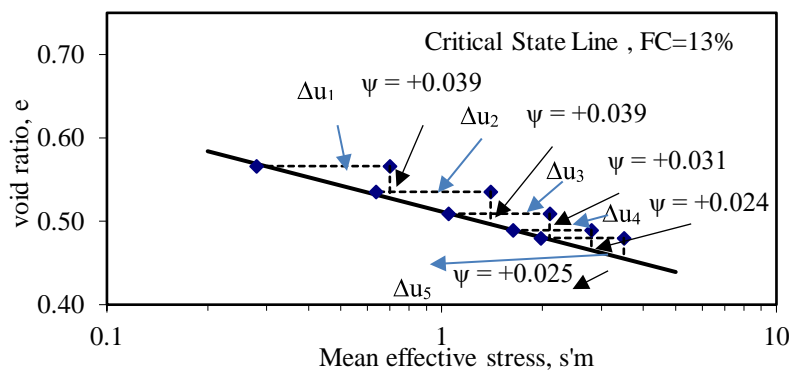


Fig. 17 Critical state line and state parameter value

The negative value of the state parameter ( $\psi = -$ ) indicates dilative soil behavior. Meanwhile, the positive state parameter value ( $\psi = +$ ) shows contradictory soil behavior, where the soil has the potential for liquefaction.

Figure 18 shows that the determination of soil behavior can be determined not only based on the void ratio but is more determined by the state parameter influenced by the void ratio and the effective stress.

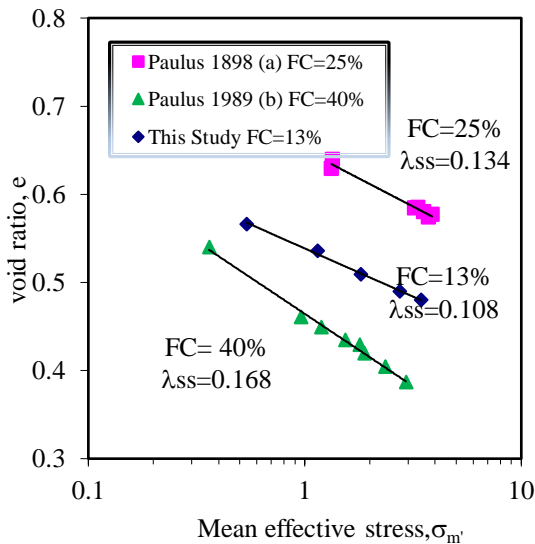


Fig. 18 The relationship between mean effective stress and void ratio

Based on Figure 18, it appears that the Fine content Fc of this Study (Palu Region) is 13%. In addition, Fc by Paulus (a) at Pepper's Ferry is 25% and Fc by Paulus (b) Yattesville is 40%. Therefore, Fc is less than Paulus (a) and Paulus (b).

In the same figure, it can be seen that the  $\lambda_{ss}$  graph is located between Paulus (a) and Paulus (b), because it is influenced by the distribution of soil grains so that the void ratio becomes smaller. So that the value  $\lambda_{ss}=0.108$  is smaller than Paulus (a)=0.168 and Paulus (b)=0.134, this is directly proportional to the percentage of fines content.

Based on the above results, the initial findings of this study are that based on laboratory test results, the sample in this study is easier for liquefaction to occur because the fine silt content (Fc) is smaller than the Paulus(a) sample and the sand content in the research sample is very high. (large with a small silt content). Therefore, further research is still needed to relate the cyclic resistance ratio to liquefaction to make the results of this study more comprehensive.

Furthermore, the research results show that an increase in fines content makes the slope of the critical state line increase so that the liquefaction resistance increases. For the Relationship between D50, Cu and  $\lambda_{ss}$ , to determine  $\psi$ , see Figure 19.

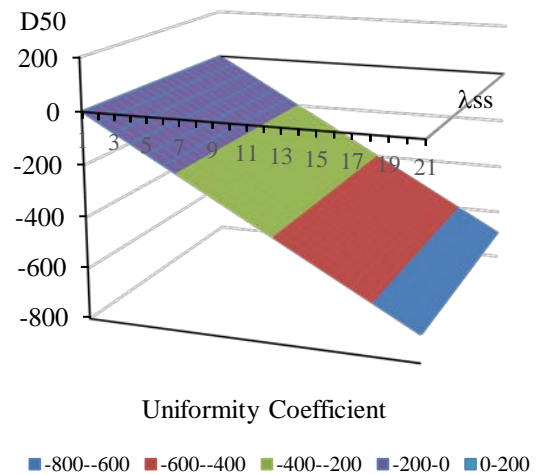


Fig. 19 The Relationship between D50, Cu and  $\lambda_{ss}$ , to determine  $\psi$

## 5. CONCLUSIONS

Liquefaction can be predicted by the state parameter, which is the proximity between the initial void ratio and the steady state line. It happened at large strain interpreted in the experimental monotonic triaxial consolidated undrained, which is highly dependent on several parameters, such as soil uniformity coefficient, fines content, relative density, and void ratio, which affect soil resistance to liquefaction.

This study has concluded the following points:

1. Grain size distribution has a significant influence on the liquefaction potential of sand with fine soil content. This is confirmed by the parameters of the uniformity coefficient (Cu), relative density (Dr) and the amount of fines contents (F.C.).
2. The liquefaction potential depends on the initial state conditions of the soil or the proximity to the steady state line. This proximity is called the state parameter, a positive state parameter indicates more susceptibility to liquefaction.
3. It is known that susceptibility to liquefaction resistance occurs in loose sand with low fines content. The potential for liquefaction will decrease with the addition of the percentage of fines content.
4. The soil under shear will lead to the steady state line, i.e., the soil flow at a constant volume and at a constant effective stress.
5. The steady-state line is a model that can describe the behavior of the soil based on the steady-state parameter, which indicates the soil is susceptible to liquefaction.
6. Soil density alone cannot describe the actual behavior of the soil because it still depends on the effective stress.

## 6. ACKNOWLEDGMENTS

The author would like to thank Universitas Islam Indonesia and the Research Team of Universitas Katholik Parahyangan for their support during this research.

## 7. REFERENCES

- [1] Jawad F.W., Al-Soud M.S., Salih M.M., Al-Ansari N., and Huda M., Liquefaction Potential of Layered Soil Under Vertical Vibration Loads. *International Journal of GEOMATE*, Vol. 23, Issue 99, 2022, pp.141–150, Retrieved from <https://doi.org/10.21660/2022.99.3470>
- [2] Yunalia M., and Nobuoto N., Seismic Properties and Fractal Dimension of Subduction Zone in Java and Its Vicinity Using Data From 1906 To 2020. *International Journal of GEOMATE*, Vol. 21, Issue 85, 2021, pp.71–83.
- [3] Almutairi F., Fat-Helbary R.E.S., Elfargawy K.O., FatahElshekh H.A., and Abd el-aal A el-aziz K., Earthquake Hazard Assessment Studies in The State of Kuwait, *International Journal of GEOMATE*, Vol. 22, Issue 90, 2022, pp.85–101
- [4] Pawirodikromo W., Makrup L., Teguh M., Anggit., Bidirectional and Directivity Effect Identifications of Synthetic Ground Motions at Selected Site In Yogyakarta City, Indonesia, *International Journal of Civil Engineering and Technology (IJCIET)*, Vol. 10, Issue 11, November 2019, pp. 149-166.
- [5] Makrup L., Sunardi B., and Muntafi Y., Design Accelerograms by Time and Frequency Domain Matching Based on Seismic Hazard in Sorowako Field of Sulawesi Island, Indonesia”, *EJGE*, Vol 21, Bund 21, pp 6629-6644.
- [6] Mina E., Kusuma R., Fathonah W., Wigati R., and Farhah A., Analysis of Soil Dynamic Response Due to Earthquake in Indonesia, *International Journal of GEOMATE Journal*, Vol. 22, Issue 91, 2022, pp.101–112.
- [7] Oliquino C.J., and Dungca J., Probabilistic Liquefaction Potential Analysis of San Fernando Pampanga, Philippines Using Semi-Markov Chain, *International Journal of GEOMATE*, Vol. 21, (87), 2021, pp.137–144.
- [8] Kazuya H., Tomohide T., Shinya T., and Atsushi I., Liquefaction Risk Assessment in the 23 Wards of Tokyo Using Elastoplastic Analysis, *International Journal of GEOMATE*, Vol. 21, Issue 86, 2021, pp.48–54.
- [9] Anda M., Purwanto S., Suryani E., Husnain., and Muchtar, Pristine Soil Property and Mineralogy as The Strategic Rehabilitation Basis in Post-Earthquake-Induced Liquefaction, Tsunami and Landslide in Palu, Indonesia. *CATENA*, 203, 105345, 2021, pp.1-16. <https://doi.org/10.1016/j.catena.2021.105345>
- [10] Ishii K., Liu W., Satoshi S., and Shoji K., Relationship Between Liquefaction Strength of Sand With Fine Fraction And Various Void Ratios, *International Journal of GEOMATE*, Vol. 22, Issue 91, 2022, pp. 1–7.
- [11] Monkul M.M., Etninan E., and Şenol A., Influence Of Content, Gradation And Shape Characteristics Of Silts On Static Liquefaction Of Loose Silty Sands, *Soil Dynamics and Earthquake Engineering*, Vol.101, 2017, pp. 12-26, <https://doi.org/10.1016/j.soildyn.2017.06.023>
- [12] Zhehao Z., Feng Z., Jean-Claude D., Jean C., Evelyne F., and Qingyun P, Assessment Of Tamping-Based Specimen Preparation Methods On Static Liquefaction Of Loose Silty Sand, *Soil Dynamics and Earthquake Engineering Journal*, Vol.143, April 2021, 106952, pp.1-10.
- [13] Ling-Yu X., Fei Cai, Wei-Yun C., Jing-Zhe Z, Dong-Dong P., Qi Wu, and Guo-Xing C., Undrained Cyclic Response Of A Dense Saturated Sand With Various Grain Sizes And Contents Of Nonplastic Fines: Experimental Analysis And Constitutive Modeling, *Soil Dynamics and Earthquake Engineering Journal*, Vol. 145, June 2021, 106727, pp.1-22.
- [14] Mehmet M.M., Sena B.K., Yunus E.T., Combined Effect Of Fines Content And Uniformity Coefficient On Cyclic Liquefaction Resistance Of Silty Sands, *Soil Dynamics and Earthquake Engineering Journal*, Vol. 151, December 2021, 106999, pp.1-14.
- [15] Ching S.C., Yibing D., Modeling For Critical State Line Of Granular Soil With Evolution Of Grain Size Distribution Due To Particle Breakage, *Geoscience Frontiers Journal*, Vol. 11, Issue 2, March 2020, pp.473-486.
- [16] Cristhian M., Márcio M.F., Critical state model for structured soil, *Journal of Rock Mechanics and Geotechnical Engineering*, Vol. 12, Issue 3, June 2020, Pages 630-64.
- [17] Hoang B.K.N., Md Mizanur R., and Andy F., The Critical State Behavior Of Granular Material In Triaxial And Direct Simple Shear Condition: A DEM Approach, *Computers And Geotechnics*, Vol. 138, 2021, 104325, pp. 1-15.
- [18] Mike J and Ken B, *Soil Liquefaction: A Critical Approach*, ISBN 0-203-30196-X Master e-book ISBN, Taylor & Francis Group, 2<sup>nd</sup> edition, 2016, pp. 401-422.
- [19] ASTM D698, Standard Test Methods for Laboratory Compaction Characteristics of Soil Using Standard Effort (12 400 ft-lbf/ft<sup>3</sup> (600 kN-m/m<sup>3</sup> ))1, PA: American Society for Testing and Materials, July 2007, pp.1-13.
- [20] Tsuchida H., Prediction and Countermeasure against Liquefaction in Sand Deposits, Seminar of the Port and Harbour Research Institute, Ministry of Transport Yokosuka Japan, 1970,

- pp. 3.1-3.33.
- [21] Hanindya K.A., Widodo P., and Edy P., Analysis of Liquefaction Potential in Volcanic Sand at Glagah Beach Kulonprogo Based on N-SPT Result. *Teknisia Journal*, 25, (2), 2020, pp.108-120.
- [22] Rahardjo P., Evaluation of Liquefaction Potential of Silty Sands Based on Cone Penetration Resistance, Dissertation submitted to the Faculty of the Virginia Polytechnic Institute and State University, 1989, pp. 79-82.
- [23] Cubrinovsk M., and Ishihara K, Maximum and Minimum Void Ratio Characteristics of Sands, *Soils and Foundations* Vol. 42, Issue. 6, pp. 65-78, December 2002 Japanese Geotechnical Society, [https://doi.org/10.3208/sandf.42.6\\_65](https://doi.org/10.3208/sandf.42.6_65)
- [24] Tokimatsu K., dan Yoshimi Y, Empirical Correlation of Soil Liquefaction Based on SPT N-Value and Fines Content, *Soils and Foundations*, Japanese Society of Soil Mechanics and Foundation Engineering, Vol.23, (4), December 1983, pp.56-74.
- [25] Monkul M.M., Etminan E., and Şenol A, Influence of coefficient of uniformity and base sand gradation on static liquefaction of loose sands with silt, *Soil Dynamics and Earthquake Engineering*, Vol. 89, 2016, pp.185–197. doi:10.1016/j.soildyn.2016.08.001
- [26] Standar Nasional Indonesia, (2004), SNI 03-2455-2004, Triaxial Test Method for Soil in Consolidated Undrained (C.U.) and Consolidated Drained (CD).
- [27] Zhu Z, Zhang F, Dupla JC, Canou J, Foerster E, (2020), Investigation On The Undrained Shear Strength Of Loose Sand With Added Materials At Various Mean Diameter Ratios. *Soil Dynamic Earthquake Engineering* ;p137. <https://doi.org/10.1016/j.soildyn.2020.106276>.
- [28] Prakash S., and Puri V.K., Liquefaction of Silts and Silt-Clay Mixtures, *Journal of Geotechnical and Geoenvironmental Engineering*, Vol. 125, Issue 8, 1999, pp. 1-27.
- [29] Cetin K.O., Seed R.B., Kayen R.E., Moss R.E.S., Bilged H.T., Ilgaca M., Chowdhury K., The Use Of The SPT-Based Seismic Soil Liquefaction Triggering Evaluation Methodology In Engineering Hazard Assessments, *MethodsX* 5, 2018, pp.1556–1575, <https://doi.org/10.1016/j.mex.2018.11.016>, 2215-0161,
- [30] Idriss I.M., Boulanger R.W., *Soil Liquefaction During Earthquakes*, Earthquake Engineering, Research Institute Monograph No:12, 2008, Earthquake Engineering Research Institute, pp.11-57.
- [31] Head K.H, and Epps R.J, *Manual of Soil Laboratory Testing Volume 3: Effective Stress Tests*, Whittles Publishing, Dunbeath Mill, Dunbeath, Caithness KW6 6EG, Scotland, UK, ISBN 978-184995-054-1, 2015, pp.59-74.
- [32] Holtz R.D., Kovacs W.D., Sheahan T.C., *An Introduction to Geotechnical Engineering*, second edition, Pearson Prentice-Hall, Inc, 1981, pp.626-662
- [33] Aude S.A., Mahmood N.S., Sulaiman S.O., Abdullah H.H., and Al Ansari N., Slope Stability and Soil Liquefaction Analysis of Earth Dams with a Proposed Method of Geotextile Reinforcement, *International Journal of GEOMATE*, Vol. 22, Issue 94, 2022, pp.102–112, Retrieved from <https://doi.org/10.21660/2022.99.3470>
- 
- Copyright © Int. J. of GEOMATE All rights reserved, including making copies unless permission is obtained from the copyright proprietors.
-